AIP | Applied Physics Letters

Controlled softening of Cu64Zr36 metallic glass by ion irradiation

K. A. Avchaciov, Y. Ritter, F. Djurabekova, K. Nordlund, and K. Albe

Citation: Appl. Phys. Lett. **102**, 181910 (2013); doi: 10.1063/1.4804630
View online: http://dx.doi.org/10.1063/1.4804630
View Table of Contents: http://apl.aip.org/resource/1/APPLAB/v102/i18
Published by the AIP Publishing LLC.

Controlled softening of $Cu_{64}Zr_{36}$ metallic glass by ion irradiation

K. A. Avchaciov,[1] Y. Ritter,[2] F. Djurabekova,[1] K. Nordlund,[1] and K. Albe[2]
[1]*Department of Physics and Helsinki Institute of Physics, University of Helsinki, Helsinki 00014, Finland*
[2]*Institut für Materialwissenschaft, TU Darmstadt, Darmstadt 564289, Germany*

(Received 21 March 2013; accepted 27 April 2013; published online 10 May 2013)

We study the effect of irradiation with 5–20 keV recoils on the topological and chemical short-range order of $Cu_{64}Zr_{36}$ metallic glass using molecular dynamics simulations. We show that within the cascade region, the structural backbone of stiff Cu-centered icosahedral units is destroyed, leading to locally softened areas. Under mechanical load, the formation of shear transformation zones is thus promoted in the damaged area. Our results suggest that irradiation is a means to introduce nucleation sites for multiple shear bands and thus prevents catastrophic failure due to the presence of a single critical shear band. © *2013 AIP Publishing LLC*. [http://dx.doi.org/10.1063/1.4804630]

Metallic glasses (MGs) exhibit unique mechanical properties like high specific strength, high hardness, and a large elastic limit.[1,2] However, their strong tendency towards strain localization, which results in macroscopically brittle failure at room temperature, limits their applicability as structural materials.[3] Recent experimental studies revealed that the mechanical properties of MGs can be improved by ion irradiation.[4–7] Depending on the projectile energy loss regime and the alloy composition, several types of structural modifications can occur. One possible consequence of ion irradiation is the precipitation of nanocrystallites in the glass matrix.[4,5] The observed increase in hardness is usually attributed to pinning of shear bands by nanocrystallites, which also, however, has been reported for non-irradiated glasses.[8]

Another effect of ion irradiation on MGs can be the destruction of the short-range order (SRO). For instance, modifications in the SRO of Fe-based metallic glasses were revealed by Mössbauer spectroscopy measurements after irradiation with Pb ions[9] and analyzed for Ni-P glass in molecular dynamics simulations (MD) of low energy cascades.[10] Since the SRO is assumed to control plastic deformation of bulk metallic glasses[11–13] it can, therefore, be expected that irradiated MGs show a modified mechanical response. Thus, the MD simulations[14] predicted a steady-state phase of CuTi MGs under the ion irradiation with the properties independent of the cooling rates during the samples preparation. Although the shear bands formation was not observed in CuTi MGs, these results are encouraging for the further investigation, especially, after the recent observation by Raghavan *et al.*[7] of the enhanced plasticity due to ion irradiation of an originally brittle Zr-based MG. The MeV ions used in this experiment produce localized damage by nuclear stopping. Here, it was assumed that the SRO was significantly damaged accompanied by an increase in free volume. This leads to a decrease in flow stress and promotes the formation of multiple shear bands, resulting in larger plasticity. Hence, in order to consider ion irradiation as a prospective approach to enhance the plasticity of MGs, a clear understanding of damage production during ion irradiation is required.

In this letter, we study the effect of ion irradiation on short-range and chemical order as well as deformation behavior of a $Cu_{64}Zr_{36}$ MG by means of molecular dynamics simulations[15] using the PARCAS code.[16] We analyze changes in local atomic structure under the influence of various irradiation conditions and simulate tensile tests to investigate the effect of ion irradiation on the mechanical properties. We observe a softening of the glassy structure after irradiation leading to an enhanced nucleation rate for shear transformation zones.

In the simulations we used an adjustable time step[17] with an upper limit of 2 fs to speed up the calculations. The interatomic interactions were described by a generalized form of the embedded-atom method (EAM) potential[18] with Mendelev's parametrization,[19] which was developed to reproduce the structural and mechanical properties of Cu-Zr glasses. The temperature was controlled towards 10 K by a Berendsen thermostat[20] coupled to atoms in the border regions of 5 nm thickness. We included the electronic stopping power as a non-local frictional force[16] applied to atoms with a kinetic energy higher than 10 eV. The electronic stopping power for Cu and Zr atoms in $Cu_{64}Zr_{36}$ alloy was calculated by the Stopping and Range of Ions in Matter (SRIM) software.[21,22]

A supercell containing about 10^6 atoms ($\sim$24 nm $\times$ 31 nm $\times$ 25 nm) was constructed by replication of a smaller cell previously obtained by slow cooling ($v_c = 0.01$ K/ps) of the molten solution. This size was chosen as a sufficiently large volume to contain the highest-energy (20 keV) collision cascades. The extent of the cascades was calculated with binary collision approximation (BCA) simulations[23] in the same material. Since we are interested in the damage produced in the atomic cascade, we focus on single cascade regions, ignited along an ion path during ion irradiation with the energy in the MeV range. The collision cascades were started by giving either a Cu or a Zr atom a recoil energy of 5 keV-20 keV. This choice is motivated by the subcascade breakdown energy being about 20 keV in dense metals,[24] i.e., higher-energy recoils would produce damage that is self-similar to that for the energies simulated here. The initial position of the recoil atoms was chosen randomly near the surface of a sphere with a radius of 20 nm; the velocity vectors were directed towards the center of the sphere. To obtain representative statistics, about 10 collision events were simulated for each initial recoil energy.

As the glass structure does not have an ordered crystalline lattice, the detection of irradiation damage becomes unintuitive. To estimate the extent of the cascades, we used the technique described in Ref. 16. Here, an atom is labelled as "liquid" if its average kinetic energy and the energy of its nearest neighbors is above a threshold energy. For crystalline solids, this threshold energy corresponds to the melting temperature by the relation $E_{liq} = \frac{3}{2}kT$. Here we used the threshold value as the melting temperature $T_m = 2400$ K of the B2 phase of Cu-Zr, which was found to give results in good agreement with the number of displaced atoms in the BCA simulations. The atoms not detected as "liquid" at any stage of a cascade evolution are considered "bulk" atoms.

Next, the structural defects produced by irradiation are analyzed using the Voronoi tessellation method.[25,26] Here, the simulation cell is divided into Voronoi polyhedra (VP) around each atom. The topology of a VP is characteristic for the local atomic structure and can be distinguished in terms of the Voronoi index $[n_3, n_4, n_5, n_6, ...]$, where n_i denotes the number of i-edged facets of the VP. Previous studies[27,28] revealed that the Cu-centered VP with index [0,0,12,0], which corresponds to the atomic structure of a full icosahedron (FI), is a key structural motif in amorphous Cu-Zr alloys. These FI units have a high packing density and shear resistance[29] and are assumed to form a structural backbone[27,28] responsible for the high strength of Cu-Zr glasses. Consequently, we characterize the topological short-range order (TSRO) by determining the fraction of Cu-centered FI units with respect to the total number of Cu atoms and changes in the TSRO by monitoring respective changes. While we obtain a FI fraction of about 24% in the as-prepared glass, the FI fraction within the cascade region after quenching is only about 15%. The fraction of all other structural motifs is not affected significantly by the irradiation events, as shown in Figure 1(a).

Figure 1(b) shows the evolution of the FI fraction during a cascade run. During the ballistic stage (up to about 10 ps), the FI fraction decreases very rapidly to 7%, but then recovers up to the final value of 15%. The recovery rates and the final FI fraction are independent of the initial recoil energy, despite the difference in the size of the damaged area. For all atoms marked as "bulk," we observe no significant changes in the FI fraction.

The chemical short-range order (CSRO) is analyzed in terms of the nearest-neighbor correlation index C_{ij}, where i and j stand for either Cu or Zr.[30] It compares the distribution of Cu- and Zr-atoms in the analyzed structure to a statistical distribution,

$$C_{ij} = \frac{p_{ij}}{p_{ij}^0} - 1.$$

Here, p_{ij} is the probability of the atoms i and j to be nearest neighbours in the analyzed structure, while the uncorrelated probability p_{ij}^0 is obtained as the number of possible permutations of ij-pairs for the total number of atoms in the system.

Changes in the CSRO during the cascade simulations are illustrated in Figure 2. Obviously, the disordering induced by a collision cascade leads to a decrease in the number of Cu–Cu and Cu–Zr bonds ($\Delta C_{Cu,Cu} \sim +0.02$; $\Delta C_{Cu,Zr} \sim -0.03$). The number of Zr–Zr bonds, on the other hand, increases ($\Delta C_{Zr,Zr} \sim +0.06$), indicating the segregation of Zr atoms. These observations are similar to what has been reported for the evolution of CSRO during plastic deformation inside a shear band in the same glassy alloy.[30] While for Cu-Cu and Cu-Zr pairs, we observe a partial recovery of the CSRO after the ballistic stage, $C_{Zr,Zr}$ remains constant. We attribute this effect to the low mobility of Zr atoms. The partial recovery of the glass structure we associate with the relatively high mobility of Cu–atoms due to radiation-induced viscous relaxation.[31] As for the TSRO

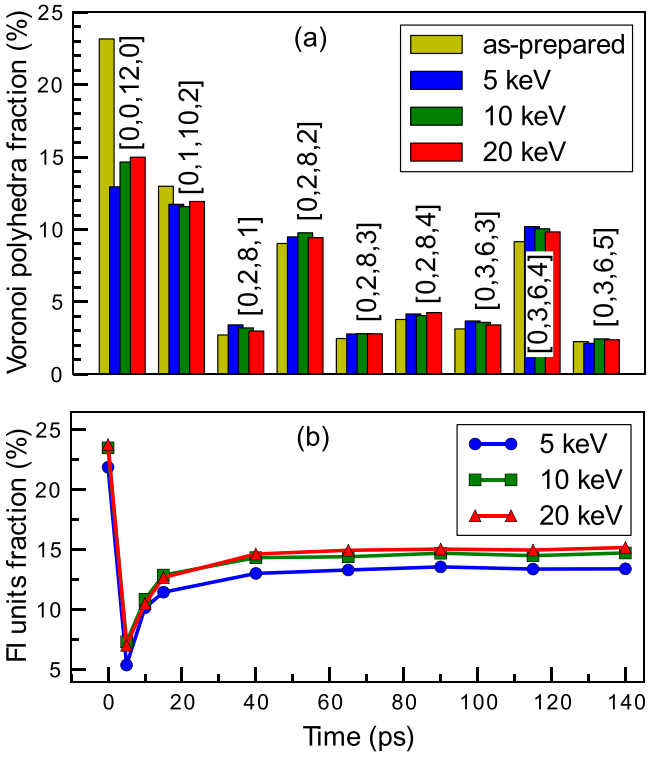

FIG. 1. (a) Fraction of Cu–centered Voronoi polyhedra with a population ≥2.5% within the cascade region before the recoil event and after the cascade was cooled down to 10 K. (b) Time evolution of the FI fraction in the cascade region for recoils with 5 keV (squares), 10 keV (circles), and 20 keV (up triangles).

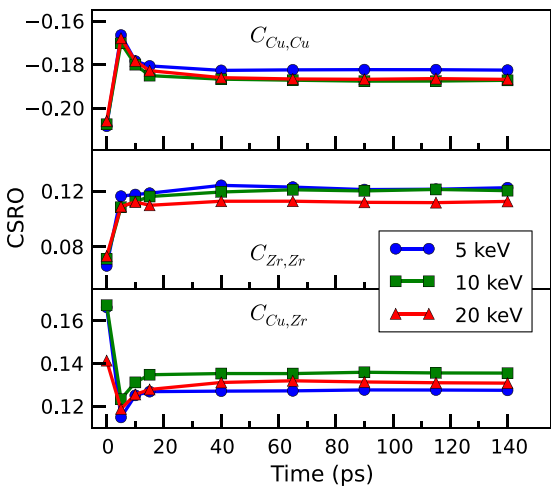

FIG. 2. Evolution of the chemical short-range order for Cu-Cu, Zr-Zr, and Cu-Zr pairs, showing that the cascade induced chemical disorder is partly recovered by more mobile Cu atoms.

results, the difference in initial recoil energy does not significantly affect the evolution of the CSRO during irradiation.

Hence, we conclude that the relative damage in TSRO and CSRO due to collision cascades is independent of the initial recoil energy, which is consistent with the results of other studies.[14,31] The latter affects only the size of the damage.

Next, to study the effect of damage accumulation in SRO, we continue irradiation of the same cell to the dose up to ~1 dpa, varying the irradiation rate. Here we take averages over three statistically independent 10 keV recoil series, each with 10 subsequent cascades, using two different irradiation rates of 100 ns^{-1} and 10 ns^{-1}. Since the damaged volume grows with every cascade, for consistency we perform the Voronoi analysis in a representative volume. This volume was chosen as a sphere of 4 nm radius placed in the box center, matching the volume of several overlapping cascades. The estimated mean size of overlap volume of the separate cascade volumes after 10 recoils does not exceed 4% of the size of the simulation cell for both rates of irradiation.

We analyze the time evolution of the FI fraction during the high dose irradiation in the same manner as in the case of the single cascades. The results are presented in Figure 3. The evolution of the FI fraction in the high irradiation rate case (100 ns^{-1}) is very similar to the one observed in the single-cascade case (cf. Figure 1(b)). Since the time between the cascades was short (no relaxation between the subsequent initial recoils), we observe a monotonic decrease of the FI fraction with the minimum of ~7% reached only by the end of the last cascade. After that, the system gradually recovers up to 15%, the same level as after a single cascade. The low irradiation rate (10 ns^{-1}) we chose such that it allows for the thermal equilibration before the following recoil is started. The time evolution of the FI fraction clearly shows a stepwise behavior, where each step corresponds to the case of the subsequent cascade. The first recoils in each series produce the highest damage: a decrease by ~1% per recoil of the total FI fraction. The relative damage produced in every following cascade is gradually decreasing and turns into zero when the FI fraction reaches the saturated value of 15%. The effect that the damage saturates is qualitatively similar to observations for crystalline metals.[32,33] On longer macroscopic timescales at room temperature, the reduction of the FI fraction from 25% to 15% will also not be significantly different, as previous studies have shown that the recovery of icosahedral units only occurs above the glass transition temperature.[30]

To summarize the analysis of the radiation effect on the atomic order, we conclude that a single cascade and multiple overlapping cascades produce similar final damage with a FI fraction around 15% (compare Figs. 1(b) and 3). Hence varying the irradiation fluence can produce either isolated damaged regions or a homogeneously damaged material, but with a similar damage level. The spatial difference in damage distribution can affect the mechanical properties in different ways.

Next we analyze the effect of ion irradiation on mechanical properties of the irradiated glass by comparing the results of the simulated uniaxial tensile tests for the irradiated (by ten cascades of 10 keV energy at the lower rate) cascades and as-prepared $Cu_{64}Zr_{36}$ MG samples. We deform the samples with a constant engineering strain rate $4 \times 10^7 s^{-1}$ along the z direction. All tensile test simulations are carried out at the constant temperature 50 K.

Figure 4(a) shows representative stress-strain curves, which we typically observe for the deformation of as-prepared and irradiated bulk samples. In the elastic regime, the behavior before and after irradiation is rather similar. Young's modulus (91.5 GPa) and the ultimate strength (4.7 GPa) decrease after the irradiation only insignificantly.

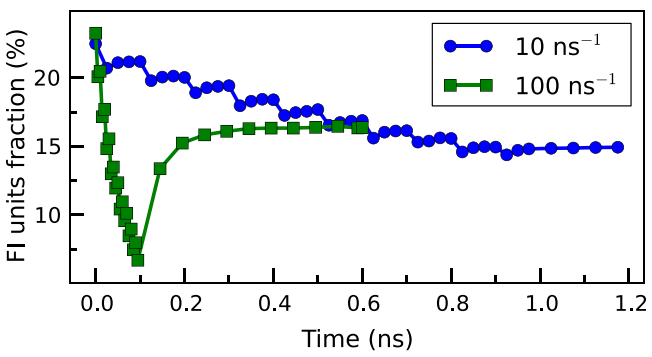

FIG. 3. Multiple 10 keV cascade simulation with different recoil rates. The results show that the accumulated damage in a larger sample volume converges to the case of a single cascade region (cf. Fig. 1(b)) for both irradiation events overlapping in time (100 ns^{-1}) and gradual damaging with thermal equilibration between the cascades (10 ns^{-1}).

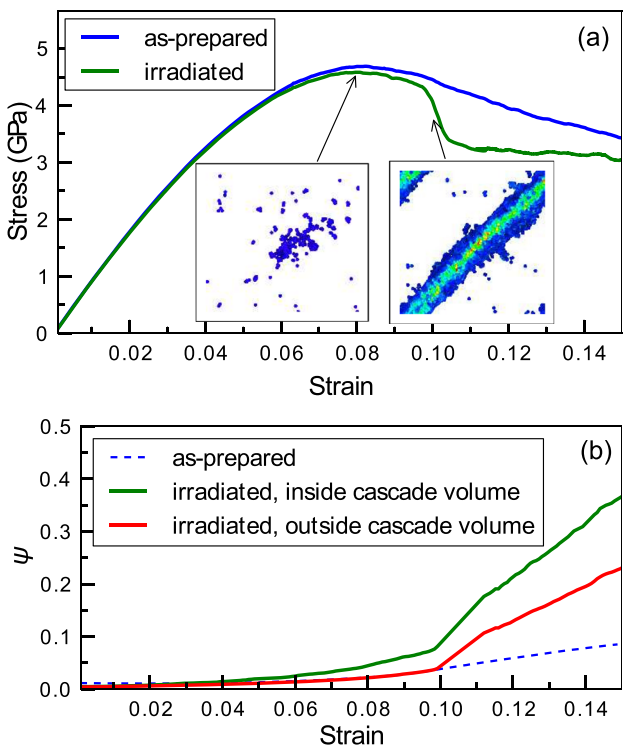

FIG. 4. (a) Representative stress-strain curves for tensile deformation of irradiated and as-prepared samples. Inset: atoms with $\eta_{Mises} > 0.2$ colored according to the atomic local shear strain; left before stress release (strain = 0.08) and right after the release (strain = 0.10). (b) Evolution of the shear localization parameter ψ during the tensile test simulations for unirradiated and irradiated samples. ψ is shown separately within the cascade volume and in the bulk not affected by the cascade.

The situation becomes different after the plastic deformation begins. The smooth decrease of the stress-strain curve in the plastic regime corresponds to the homogeneous plastic flow in the unirradiated sample. The significant stress drop just after the maximum observed in irradiated sample corresponds to the formation of a mature shear band.

The details of shear banding become clear by calculating the atomic local shear strain η_{Mises}.[34,35] Inspecting the atomic-level von Mises strain, we observe a homogeneous distribution of shear transformation zones in the unirradiated sample, whereas the irradiated sample exhibits an increased nucleation rate of shear transformation zones and thus the formation of an embryonic shear band in the cascade volume, as illustrated in Fig. 4(a), left inset. The complete shear banding is illustrated in the right inset of Fig. 4(a), which shows the atomic von Mises strains after the stress was released.

The irradiation-induced transition from homogeneous to inhomogeneous deformation can be also seen from the shear localization parameter,[36]

$$\psi = \sqrt{\frac{1}{N}\sum_{i=1}^{N}(\eta_i^{\mathrm{Mises}} - \eta_{\mathrm{ave}}^{\mathrm{Mises}})^2},$$

where $\eta_{\mathrm{ave}}^{\mathrm{Mises}}$ is the average von Mises strain over all atoms in the simulation cell. We analyze this parameter separately for the cascade-affected and bulk regions of the irradiated sample, and compare with ψ in the unirradiated sample. The results (Fig. 4(b)) support the view that shear events start within the cascade area (where ψ is the highest) and propagate into the matrix leading to strain localization in a single shear band. In the unirradiated sample, the ψ parameter stays low, indicating homogeneous deformation behavior.

Our results correlate well with the results reported in Refs. 14 and 31. However, in our work we observe promotion of shear band formation by irradiation, while the previously studied CuTi[14] and NiP[10] MGs did not show such behavior.

In summary, we study the effect of ion irradiation on $Cu_{64}Zr_{36}$ metallic glass using molecular dynamics simulations. We find that low energy collision cascades initiated by ion irradiation damage the topological and chemical short-range order in the glassy alloy, but that the fraction of full icosahedral units during prolonged irradiation is insensitive to initial recoil energy, dose, and flux. We further show that within the cascade region, the structural backbone of stiff Cu-centered icosahedral units is destroyed, leading to locally softened areas. Under mechanical load, the formation of shear transformation zones is thus promoted in the damaged area. Our results imply that in a macroscopic irradiation situation, by selecting a fluence which produces spatially separated damage regions, one could control the volume density of damaged regions and hence the number of nucleation sites to enable forming multiple interacting shear bands, which can enhance the ductility of metallic glasses.

The results of the work were obtained using computational resources of MCC NRC "Kurchatov Institute" (http://computing.kiae.ru/) and CSC-IT Center for Science Ltd. We acknowledge financial support from the National Graduate School in Materials Physics in Finland, the Academy of Finland, the DFG through Project No. AL-578/13 and a DAAD-PPP travel grant.

[1]C. A. Schuh, T. C. Hufnagel, and U. Ramamurty, Acta Mater. **55**, 4067 (2007).
[2]J. Eckert, J. Das, S. Pauly, and C. Duhamel, J. Mater. Res. **22**, 285 (2007).
[3]M. F. Ashby and A. L. Greer, Scr. Mater. **54**, 321 (2006).
[4]J. Carter, E. Fu, M. Martin, G. Xie, X. Zhang, Y. Wang, D. Wijesundera, X. Wang, W.-K. Chue, and L. Shao, Scr. Mater. **61**, 265 (2009).
[5]W. Luo, B. Yanga, and G. Chen, Scr. Mater. **64**, 625 (2010).
[6]J. Carter, E. Fu, G. Bassiri, B. Dvorak, N. D. Theodore, G. Xie, D. Lucca, M. Martin, M. Hollander, X. Zhang, and L. Shao, Nucl. Instrum. Methods Phys. Res. B **267**, 1518 (2009).
[7]R. Raghavan, K. Boopathy, R. Ghisleni, M. Pouchon, U. Ramamurty, and J. Michler, Scr. Mater. **62**, 462 (2010).
[8]S. Pauly, S. Gorantla, G. Wang, U. Kuhn, and J. Eckert, Nature Mater. **9**, 473 (2010).
[9]M. Kopcewicza and A. Dunlop, J. Appl. Phys. **90**, 74 (2001).
[10]T. Mattila, R. Nieminen, and M. Dzugutov, Nucl. Instrum. Methods Phys. Res. B **102**, 119 (1995).
[11]A. L. Greer and E. Ma, MRS Bull. **32**, 611 (2007).
[12]M. W. Chen, Annu. Rev. Mater. Res. **38**, 445 (2008).
[13]Y. Q. Cheng and E. Ma, Prog. Mater. Sci. **56**, 379 (2011).
[14]S. Mayr, Phys. Rev. B **71**, 144109 (2005).
[15]M. P. Allen and D. J. Tildesley, *Computer Simulation of Liquids* (Oxford University Press, Oxford, 1989).
[16]K. Nordlund, M. Ghaly, R. S. Averback, M. Caturla, T. Diaz de la Rubia, and J. Tarus, Phys. Rev. B **57**, 7556 (1998).
[17]K. Nordlund, Comput. Mater. Sci. **3**, 448 (1995).
[18]S. M. Foiles, M. I. Baskes, and M. S. Daw, Phys. Rev. B **33**, 7983 (1986); *ibid.* **37**, 10378 (1988).
[19]M. I. Mendelev, D. K. Rehbein, R. T. Ott, M. J. Kramer, and D. J. Sordelet, J. Appl. Phys. **102**, 093518 (2007).
[20]H. J. C. Berendsen, J. P. M. Postma, W. F. van Gunsteren, A. DiNola, and J. R. Haak, J. Chem. Phys. **81**, 3684 (1984).
[21]J. F. Ziegler, J. P. Biersack, and M. D. Ziegler, *SRIM – The Stopping and Range of Ions in Matter* (SRIM Co., Chester, Maryland, USA, 2008).
[22]J. F. Ziegler, SRIM-2008 software package, available online at http://www.srim.org.
[23]T. S. Pugacheva, F. G. Djurabekova, and S. K. Valiev, Nucl. Instrum. Methods Phys. Res. B **141**, 99 (1998).
[24]K. Nordlund, L. Wei, Y. Zhong, and R. S. Averback, Phys. Rev. B **57**, R13965 (1998).
[25]C. H. Rycroft, G. S. Grest, J. W. Landry, and M. Z. Bazant, Phys. Rev. E **74**, 021306 (2006).
[26]C. H. Rycroft, "Multiscale Modeling in Granular Flow," Ph.D. dissertation, Massachusetts Institute of Technology (2007).
[27]Y. Cheng, H. Sheng, and E. Ma, Phys. Rev. B **78**, 014207 (2008).
[28]M. Li, C. Z. Wang, S. G. Hao, M. J. Kramer, and K. M. Ho, Phys. Rev. B **80**, 184201 (2009).
[29]J.-C. Lee, K.-W. Park, K.-H. Kim, E. Fleury, B.-J. Lee, M. Wakeda, and Y. Shibutani, J. Mater. Res. **22**, 3087 (2007).
[30]Y. Ritter and K. Albe, Acta Mater. **59**, 7082 (2011).
[31]S. G. Mayr, Y. Ashkenazy, K. Albe, and R. S. Averback, Phys. Rev. Lett. **90**, 055505 (2003).
[32]R. S. Averback and K. L. Merkle, Phys. Rev. B **16**, 3860 (1977).
[33]K. Nordlund and R. S. Averback, Phys. Rev. B **56**, 2421 (1997).
[34]A. Stukowski, Modell. Simul. Mater. Sci. Eng. **18**, 015012 (2010).
[35]F. Shimizu, S. Ogata, and J. Li, Acta Mater. **54**, 4293 (2006).
[36]A. J. Cao, Y. Q. Cheng, and E. Ma, Acta Mater. **57**, 5146 (2009).